Supramolecular nanostructures that mimic VEGF as a strategy for ischemic tissue repair

Matthew J. Webber[a,1], Jörn Tongers[b,c,1], Christina J. Newcomb[d], Katja-Theres Marquardt[b], Johann Bauersachs[c], Douglas W. Losordo[b,1,2], and Samuel I. Stupp[d,e,f,g,1,2]

[a]Department of Biomedical Engineering, Northwestern University, Evanston, IL 60208; [b]Feinberg Cardiovascular Research Institute, Feinberg School of Medicine, Northwestern University, Chicago, IL 60611; [c]Cardiology and Angiology, Hannover Medical School, 30625 Hannover, Germany; [d]Department of Materials Science and Engineering, Northwestern University, Evanston, IL 60208; [e]Department of Chemistry, Northwestern University, Evanston, IL 60208; [f]Department of Medicine, Northwestern University, Chicago, IL 60611; and [g]Institute for Bionanotechnology in Medicine, Chicago, IL 60611

Edited by David A. Tirrell, California Institute of Technology, Pasadena, CA, and approved July 7, 2011 (received for review November 3, 2010)

There is great demand for the development of novel therapies for ischemic cardiovascular disease, a leading cause of morbidity and mortality worldwide. We report here on the development of a completely synthetic cell-free therapy based on peptide amphiphile nanostructures designed to mimic the activity of VEGF, one of the most potent angiogenic signaling proteins. Following self-assembly of peptide amphiphiles, nanoscale filaments form that display on their surfaces a VEGF-mimetic peptide at high density. The VEGF-mimetic filaments were found to induce phosphorylation of VEGF receptors and promote proangiogenic behavior in endothelial cells, indicated by an enhancement in proliferation, survival, and migration in vitro. In a chicken embryo assay, these nanostructures elicited an angiogenic response in the host vasculature. When evaluated in a mouse hind-limb ischemia model, the nanofibers increased tissue perfusion, functional recovery, limb salvage, and treadmill endurance compared to controls, which included the VEGF-mimetic peptide alone. Immunohistological evidence also demonstrated an increase in the density of microcirculation in the ischemic hind limb, suggesting the mechanism of efficacy of this promising potential therapy is linked to the enhanced microcirculatory angiogenesis that results from treatment with these polyvalent VEGF-mimetic nanofibers.

Ischemic tissue disease remains one of the foremost causes of morbidity and mortality worldwide (1). There is tremendous need for new therapeutic approaches that regenerate ischemic tissue. One target is to enhance microvasculature perfusion in ischemic tissue by delivering proangiogenic signals, termed therapeutic angiogenesis. The mechanisms of angiogenesis have been extensively studied and its regulation involves complex cascades of signaling molecules and growth factors (2). VEGF is among the most potent, yet rate limiting, of these angiogenic factors (3). Thus, efforts toward therapeutic angiogenesis have focused on VEGF to enhance microvasculature in ischemic tissue. However, clinical trials to date have not convincingly demonstrated efficacy (4, 5). One potential obstacle for the success of these therapies is inadequate retention of protein in the target zone because protein retention in tissue is on the order of minutes to hours, depending on delivery route (6–8). Maintaining a therapeutic level of protein within ischemic tissue could require serial treatments over time, making these therapies more invasive and necessitating cost-prohibitive quantities of protein (4).

Recent work has demonstrated the therapeutic potential of a platform of self-assembling filamentous nanofibers formed from customizable peptide amphiphile (PA) molecules (9–12). PAs consist of a hydrophobic alkyl segment covalently linked to a peptide sequence that contains at least two domains: an amino acid sequence that drives self-assembly of the molecules into nanofibers through the formation of β-sheets and a customizable bioactive domain designed to interact with specific proteins, receptors, biopolymers, or other cellular targets. Hydrophobic collapse drives the alkyl tails into the core of the nanofiber, resulting in the presentation of the bioactive domain on the fiber surface. These nanofibers have dimensions similar to filamentous structures in the extracellular matrix and can form gel networks at low concentrations in aqueous media, allowing for three-dimensional entrapment of cells presuspended in aqueous PA solutions (13). Their high aspect ratio and the high surface area of displayed signals at controlled density likely facilitate their enhanced biological signaling, while their extensive internal hydration also offers the necessary dynamics to promote interaction with receptors and ligands (14–16). Furthermore, these PA-based therapies can be delivered noninvasively as easily injectable liquids that become solid nanostructures in situ and are biocompatible with desirable rates of degradation and tissue clearance over a period of weeks (17–19).

Advancements in the design of biomaterials have enabled some of the issues of bolus VEGF protein therapy to be overcome through the use of materials to control the spatial and temporal delivery of VEGF (20). These scaffolds have been designed to control the release kinetics through scaffold design (21–23), the use of heparin to specifically bind VEGF (24, 25), or through the covalent attachment of VEGF for on-demand cell-mediated VEGF delivery (26, 27), among many other strategies. The general concept aims to use materials to control the kinetics of protein bioavailability. However, each strategy is reliant on recombinant proteins and, although some are injectable, some require invasive surgical implantation within the site where angiogenesis is to be modulated. In addition, a number of synthetic strategies have emerged to modulate angiogenesis through small molecules or peptides and have been developed to antagonize receptors for cancer therapies or to promote angiogenesis by signaling through these receptors (28, 29). Currently, only one synthetic oligopeptide has been demonstrated to mimic VEGF through the activation of its receptors (30, 31). This peptide was designed based on the native α-helical receptor-binding domain of VEGF and was shown to mimic native VEGF through activation of VEGF receptors. This synthetic approach, although potentially addressing issues related to the production of recombinant proteins, does not address the poor tissue retention for protein-based therapies.

Here, the customizable presentation of bioactive signals on our PA platform was leveraged to present this VEGF-mimetic epitope in a polyvalent fashion on the surface of high aspect ratio nanofibers. This strategy could provide a feasible synthetic

Author contributions: M.J.W., J.T., J.B., D.W.L., and S.I.S. designed research; M.J.W., J.T., C.J.N., and K.-T.M. performed research; M.J.W. and J.T. analyzed data; and M.J.W., J.T., D.W.L., and S.I.S. wrote the paper.

The authors declare no conflict of interest.

This article is a PNAS Direct Submission.

[1]M.J.W. and J.T. contributed equally to this work.

[2]To whom correspondence may be addressed: E-mail: s-stupp@northwestern.edu or d-losordo@northwestern.edu.

This article contains supporting information online at www.pnas.org/lookup/suppl/doi:10.1073/pnas.1016546108/-/DCSupplemental.

alternative to protein therapies that would address issues of tissue retention and bioavailability. Moreover, polyvalent epitope display could enhance the dimerization-dependent signaling of the VEGF receptors. Thus, we have evaluated here PA presentation of this VEGF-mimetic sequence and its possible use as therapy for ischemic tissue regeneration.

Results

Design and Characterization of a VEGF-Mimetic PA. The VEGF PA (Fig. 1*A*) was designed to display on the surface of nanostructures a peptide sequence that mimics VEGF, KLTWQELYQLKYKGI-NH_2 (30). At the N terminus of this peptide, we covalently attached a K_3G sequence to facilitate solubility and a V_2A_2 β-domain followed by a C_{16} alkyl chain to promote self-assembly into cylindrical nanostructures through intermolecular hydrogen bonding and hydrophobic collapse (Fig. 1*G*). Cryogenic transmission electron microscopy (TEM) of this PA reveals the formation of self-assembled high aspect ratio cylindrical nanostructures (Fig. 1*B*). At a concentration used for therapeutic studies and in the presence of divalent counterions, VEGF PA nanostructures form entangled nanofiber gels (Fig. 1*C*). The reported bioactive secondary structure of the VEGF-mimetic sequence is α-helical (30, 31). CD of the VEGF PA revealed a signal characteristic of α-helix (Fig. 1*D*). This α-helix had greater conformational stability when incorporated in PA molecules (Fig. 1*E*) compared to the peptide alone (Fig. 1*F*), evident by less change in the 220-nm α-helical CD signature upon heating. Conjugation to an alkyl tail is known to stabilize α-helical peptides (32) and supramolecular effects could also explain the increased thermal stability of the α-helical epitope when presented on the PA. Such stabilization of the bioactive conformation of the peptide by PA conjugation could enhance the potency of the epitope. In addition to the VEGF PA and epitope-only peptide control, a PA was synthesized with systematic replacement of four specific residues known to be near the peptide–receptor-binding interface with structurally distinct amino acids. Structures of all molecules used in this study are shown (Fig. S1).

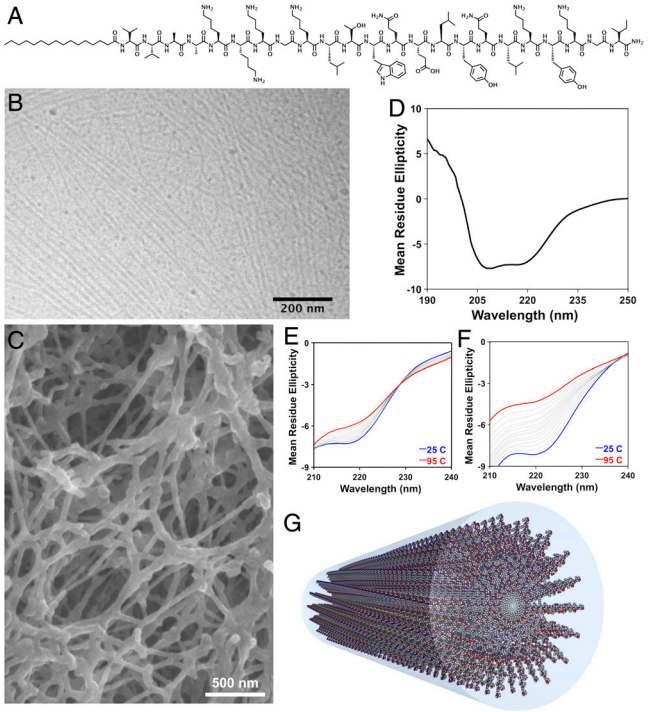

Fig. 1. The chemical structure of the VEGF-mimetic peptide amphiphile (*A*), designed to assemble into cylindrical nanostructures (*G*). The VEGF PA forms nanofibers, visualized by cryogenic TEM (*B*), and entangled nanofiber gel networks, imaged by SEM (*C*). Circular dichroism for the VEGF PA demonstrating α-helical secondary structure (*D*), and melting analysis performed about the 220-nm α-helical signature for VEGF PA (*E*) and the peptide epitope control (*F*).

VEGF PA Specifically Activates VEGF Receptors in Vitro. VEGF signal transduction is initiated by phosphorylation of several tyrosines on the intracellular receptor domain (33). In order to determine VEGF-mimetic signaling of the VEGF PA, human umbilical vein endothelial cells (HUVECs) were stimulated with VEGF PA and then quantified for the amount of phosphorylated VEGF receptor 1 (VEGFR1) or phosphorylated VEGF receptor 2 (VEGFR2), the two primary VEGF receptors implicated in its angiogenic signaling. Stimulation with the VEGF PA resulted in an amount of phosphorylated VEGFR1 (Fig. 2*A*) that was 1.63 times greater than an untreated control group ($P < 0.001$), showing a significant enhancement in receptor phosphorylation. Interestingly, the level of phosphorylation for the VEGF PA was also significantly greater than for the bioactive VEGF peptide ($P < 0.001$) and mutant PA ($P < 0.001$). The bioactive peptide also induced significantly greater phosphorylation than untreated controls. For VEGFR2 phosphorylation (Fig. 2*B*), the VEGF PA (1.58 times increase) again demonstrated phosphorylation levels significantly greater than an untreated control ($P < 0.001$). The value for the VEGF peptide was again less than that for the VEGF PA. The mutant PA again demonstrated no effect on VEGFR2 phosphorylation, establishing this as an ideal material control for the VEGF PA. Both the VEGF PA and the VEGF peptide signal similarly to the VEGF assay control for both

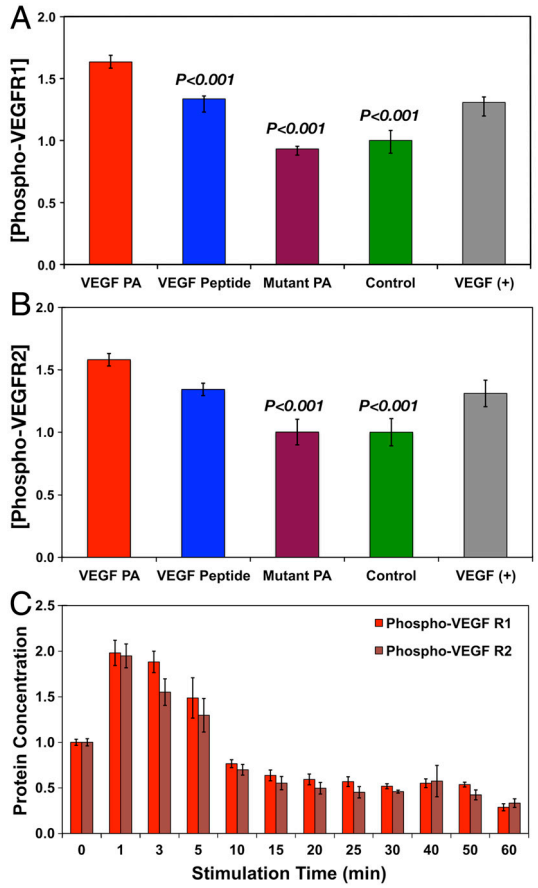

Fig. 2. Results from an ELISA assay for the receptor phosphorylation of VEGFR1 (*A*) and VEGFR2 (*B*) as well as a time course of phosphorylation for both VEGFR1 and VEGFR2 (*C*). Significance is shown relative to VEGF PA treatment. VEGF protein is shown as an assay control for verification of phosphorylation and was not included in statistical analysis as a comparative group.

receptors, confirming reports on the discovery of the epitope (30). Examining the effect of VEGF PA stimulation over time (Fig. 2*C*), we observed an initial rise in the levels of both phosphorylated VEGFR1 and VEGFR2, followed by a decrease beginning at 10 min of stimulation to levels below the baseline of an untreated control. The response and time frame of signaling by VEGF PA is consistent with the known temporal response for VEGF receptor activation followed by subsequent cleavage of phosphates and ubiquitination of the receptor (34).

VEGF signaling is known to enhance, among other cellular functions, the proliferation, survival, and migration of endothelial cells (3, 33). Therefore we also evaluated these phenotypic outcomes in HUVECs upon exposure to VEGF PA (Fig. S2). Prolonged stimulation with VEGF PA significantly increased cell number 1.37 times compared to an untreated control ($P < 0.001$). In addition, HUVECs that were serum-starved exhibited significantly improved survival in the presence of the VEGF PA (10.2% apoptotic) compared to an untreated group (31.7% apoptotic, $P < 0.001$). Neither the VEGF peptide nor the mutant PA group significantly enhanced cell number or survival. In addition, treatment with VEGF PA resulted in a significant increase in migration into a denuded scratch (68.7% closure) compared to an untreated control (25.2% closure, $P < 0.05$), whereas treatment with the VEGF peptide did not significantly enhance migration relative to the untreated control group.

The robust effect on HUVEC function in vitro, combined with VEGF-specific receptor phosphorylation, supports the VEGF-mimetic activity of the VEGF PA nanofibers. The VEGF peptide, meanwhile, did not show similar effects on endothelial cell function in vitro in spite of a demonstrated increase in receptor phosphorylation. As the phosphorylation studies were performed for only a single phosphorylation cycle, it is possible that the peptide does not retain potency over longer times in culture. Alternatively, it could be that the incremental increase in phosphorylation by VEGF PA compared to the VEGF peptide seen in one phosphorylation cycle results in a cumulative effect on cell activity over the time course of many phosphorylation cycles afforded by longer functional in vitro experiments.

VEGF PA Induces Angiogenesis in Vivo. An established in vivo angiogenesis model, the chicken chorioallantoic membrane (CAM) assay, was used to evaluate the angiogenic activity of the VEGF PA. When VEGF PA was coated onto a glass coverslip and applied to the CAM (Fig. 3), we saw a 229% increase in the blood vessel density over the following 3 d. For comparison, this increase was significantly greater ($P < 0.001$) than CAM treated with the VEGF peptide (139%), mutant PA (149%), or saline (132%). This result suggests a strong angiogenic response from treatment with the VEGF PA. This effect is visualized in the density of blood vessels at the point of CAM stimulation, in addition to indications of vascular remodeling and leakage and the spoke-like pattern radiating from the center of the coverslip where the material was applied. Representative images from the various controls do not display a similar effect. This assay confirms the angiogenic properties of our VEGF PA using an in vivo model and reinforces proangiogenic findings in vitro.

VEGF PA Enhances Repair of Ischemic Hind-Limb Tissue. The murine hind-limb ischemia model was used to evaluate the potential of the VEGF-mimetic PA nanostructures as a therapy for ischemic disease. VEGF PA or control treatments were administered by an intramuscular injection 3 d after the induction of critical ischemia by ligation and excision of the right femoral artery and all superficial and deep branches. To assess functional recovery after critical hind-limb ischemia, animals were assessed for limb salvage and limb motor function via established semiquantitative scoring methods. In terms of tissue necrosis and amputation of ischemic limb, we saw significant improvement ($P < 0.05$) in

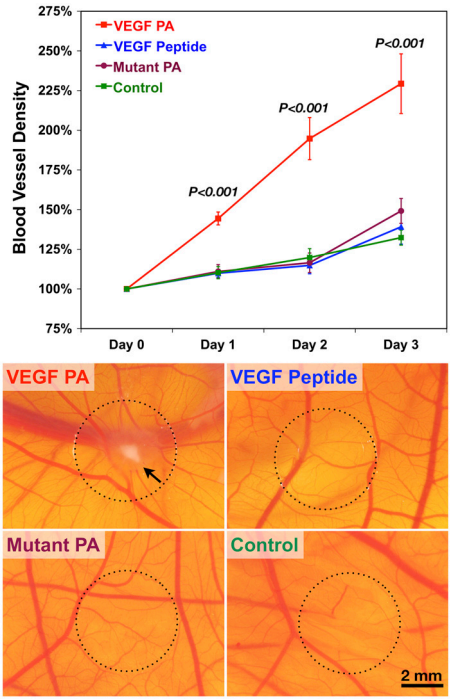

Fig. 3. Quantified results from the CAM assay beginning on embryonic day 10 (t = day 0) and extending for 4 d along with representative images from day 3 for treatments of VEGF PA, VEGF peptide, mutant PA, and an untreated control. Significance shown is for VEGF PA treatment compared to all other treatment groups. The scale bar shown corresponds to 2 mm in all micrographs.

tissue salvage (i.e., less necrosis) in animals treated with VEGF PA (Fig. 4*A*) at both day 21 and day 28 compared to animals treated with VEGF peptide, mutant PA, and saline. When scoring animals based on active limb motor function (Fig. 4*B*), we again saw a significant effect for treatment with the VEGF PA at day 21 ($P < 0.05$) and day 28 ($P < 0.01$) compared to treatment with the VEGF peptide, mutant PA, and saline. This assessment of limb use suggests that treatment with the VEGF PA leads to a more functional phenotype, which was further supported in results subjecting animals to a walking endurance test using a Rota Rod treadmill at day 28 (Fig. 4*C*). Animals treated with VEGF PA walked significantly longer prior to failure (150.5 s) than animals treated with the VEGF peptide (115.6 s, $P < 0.05$), mutant PA (106.7 s, $P < 0.05$), and saline (90.4 s, $P < 0.001$).

Laser Doppler perfusion imaging (LDPI) was performed to assess tissue perfusion in the ischemic hind limb (Fig. 4*D*). Treatment with VEGF PA significantly enhanced the recovery of tissue perfusion following treatment. At 14 d after induction of ischemia, animals treated with VEGF PA had a perfusion ratio (0.76) significantly greater than that for animals treated with the VEGF peptide (0.54, $P < 0.01$), mutant PA (0.42, $P < 0.01$), or a control injection of saline (0.53, $P < 0.05$). At day 28, animals treated with VEGF PA continued to have a significantly higher perfusion ratio (0.72) than animals treated with the VEGF peptide (0.52, $P < 0.05$), mutant PA (0.48, $P < 0.05$), and saline (0.52, $P < 0.05$).

Histological tracking of fluorescently tagged PA and peptide in muscle tissue of the ischemic hind limb revealed that the PA is retained significantly longer than the peptide control (Fig S3). Harvesting ischemic limb tissue at 2, 7, and 14 d after administration of treatment revealed large quantities of VEGF PA remained in the ischemic hind limb. Even small quantities could be seen at 28 d after treatment. A thorough histological search for fluorescently tagged VEGF peptide did not indicate any material remained in the tissue at any of these follow-up points. It is known

that proteins, such as VEGF, have short retention times in tissue (6–8). The enhanced retention observed for VEGF PA could underlie its therapeutic benefit compared to the peptide epitope control.

In order to determine whether the beneficial effects of VEGF PA treatment on recovery of blood flow, motor function, and tissue salvage were associated with an effect on the microcirculation of the ischemic limb muscle, we quantified the number of $CD31^+$ capillaries in the ischemic limb harvested at day 28 (Fig. 5). There was a significant increase in the number of $CD31^+$ capillaries in animals treated with VEGF PA (1,582/mm^2) compared to treatment with VEGF peptide (949/mm^2, $P < 0.001$), mutant PA (954/mm^2, $P < 0.001$), and saline (893/mm^2, $P < 0.001$). This proangiogenic effect of VEGF PA on the microcirculation is consistent with its angiogenic activity in the CAM assay, and reinforces its therapeutic efficacy for ischemic tissue repair. Of note, there was no effect on the number of $CD31^+$/smooth muscle actin+ arterioles, also known as muscularized or mature capillaries. VEGF protein treatment can result in the development of immature vasculature, and this is one known limitation surrounding VEGF therapy (35). We do not know at this time if a lack of mature capillaries will be a limitation in the translation of VEGF PA. However, the versatility of supramolecular PA systems allows for multiplexing of bioactive signals, and future efforts could explore the development of PA mimics of other growth factors (i.e., FGF-2) that, in combination with VEGF signaling, are known to promote more mature vasculature.

Overall, the improvements in tissue perfusion, limb salvage, motor function, and capillarization point to the therapeutic utility of VEGF PA for ischemic tissue repair. Thus, VEGF PA nanostructures are identified here as a promising synthetic therapeutic strategy for ischemic cardiovascular disease.

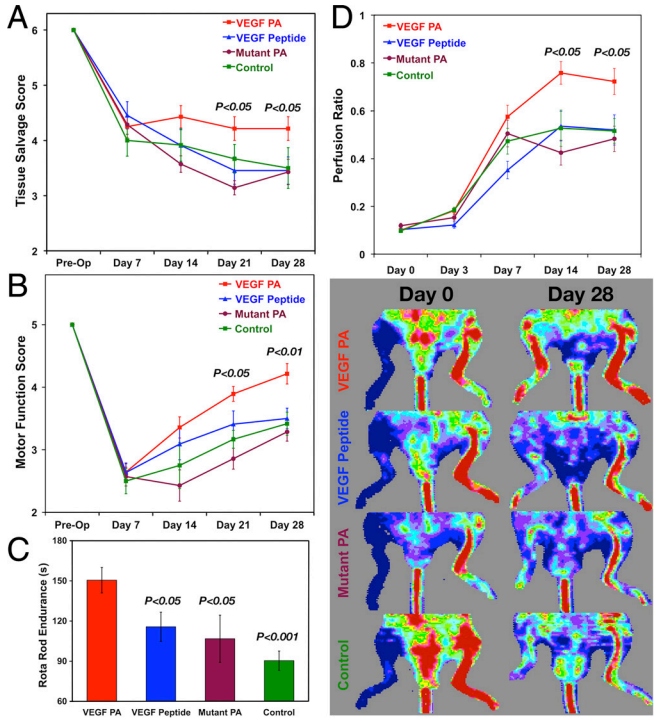

Fig. 4. Results from in vivo hind-limb ischemia study examining the tissue salvage score (*A*) and the motor function score (*B*) of the various treatment groups over time, as well as the endpoint analysis at day 28 of failure time for a Rota Rod motor functional performance test (*C*). Laser Doppler perfusion imaging (*D*) for mouse hind-limb ischemia studies quantified as the perfusion ratio of treated to untreated limb along with representative LDPI images from the same animal at day 0 and day 28 for treatments of VEGF PA, VEGF peptide, mutant PA, and an untreated control. Significance is shown for the VEGF PA relative to other treatments (*A*, *B*, and *D*) and for other treatments compared to the VEGF PA treatment (*C*).

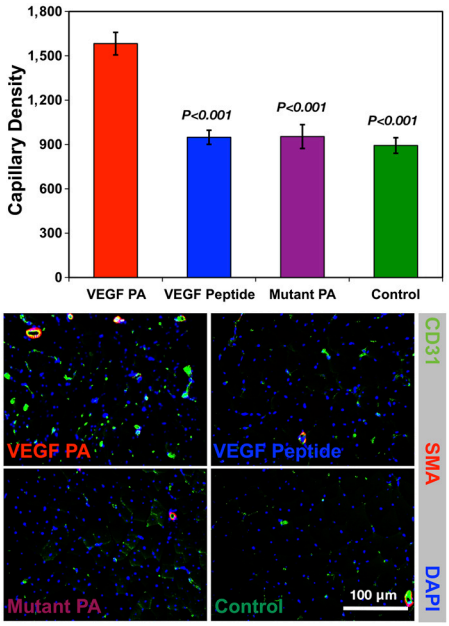

Fig. 5. Results from quantification of immunohistological staining for $CD31^+$ capillary forms in the ischemic tissue at day 28 of the hind-limb ischemia study, as well as representative immunohistological images staining for CD31 (green), smooth muscle α-actin (red), and nuclei (blue) for treatments of VEGF PA, VEGF peptide, mutant PA, and an untreated control. Significance is shown relative to VEGF PA treatment, and the scale bar shown corresponds to 100 μm in all micrographs.

Although the primary objective of this work was to establish that supramolecular epitope display could enhance the potency of a VEGF-mimetic epitope, it remained of interest to see how this PA therapy would compare to a recombinant protein approach. Thus, following up on the promising therapeutic potential demonstrated, a second in vivo study comparing the VEGF PA to a bioactive treatment of $VEGF_{165}$ protein in the ischemic hind limb was performed (Fig. S4). Because there exists no literature consensus on an effective dose of VEGF protein for intramuscular delivery in a mouse ischemic hind limb, and to be sure that an effective protein dose was used, a relatively high dose of 20 μg per animal was selected. For comparison, intramuscular delivery of 3 μg was shown to be ineffective in a mouse hind-limb model when delivered as a bolus without a biomaterial to control its release (21), whereas a 50-μg intramuscular bolus was effective in a similar model in much larger rats (*ca.* 300 g) (36). For these studies, the control group receiving a saline injection and the group receiving VEGF PA were repeated to account for variability in the model or in instrumentation for functional assessment. As shown, both the VEGF PA and $VEGF_{165}$ performed similarly on the basis of LDPI perfusion ratio, with both showing a significant increase ($P < 0.05$) compared to the control (Fig. S4*A*). Scoring for limb necrosis indicated that only the VEGF PA group significantly ($P < 0.05$) enhanced tissue salvage compared to the control, with a trend for improvement in the VEGF protein group that was not significant from the control (Fig. S4*B*). Scoring for motor function in the hind limb indicated that both the VEGF PA group ($P < 0.01$) and the VEGF protein group ($P < 0.05$) significantly improved limb motor function compared to the control group (Fig. S4*C*). The measure that was most affected by VEGF PA treatment was histological capillary density in the ischemic hind-limb muscle. Treatment with VEGF PA resulted in significantly ($P < 0.001$) more capillaries in the hind limb than for treatment with either VEGF protein or the control (Fig. S4*D*). VEGF protein also demonstrated a significant ($P < 0.001$)

increase in capillary density compared to the control. This dramatic effect in capillarization could result from the prolonged retention and activity of the VEGF PA in the muscle tissue compared to the VEGF protein. Overall, the robust therapeutic effect seen previously for VEGF PA was conserved in these studies and the PA performed as well or better than the recombinant protein in every measured outcome.

Discussion

Here we have demonstrated the use of bioactive and biodegradeable nanostructures as a strategy for therapeutic angiogenesis. The display on the surface of these nanofibers of a peptide mimic of VEGF showed enhanced signaling and bioactivity by activation of specific VEGF receptors and consequent functional outcomes for endothelial cells in vitro. The proangiogenic activity of this system was further substantiated in vivo using the CAM assay. Evaluation of the therapeutic potential of these VEGF PA nanostructures in a murine hind-limb ischemia model revealed improved tissue perfusion, limb motor function, limb salvage, and capillarization of the ischemic limb. The demonstrated efficacy suggests further consideration of these systems as an alternative therapy to protein-based strategies currently being evaluated for ischemic cardiovascular diseases.

The material we have evaluated here is similar to that demonstrated previously with a different class of self-assembling peptides, where a VEGF-mimetic epitope and a cell adhesion epitope (RGDS) were evaluated for their ability to promote proliferation, migration, and tubulogenesis of cultured HUVECs (37). In this previous study, the VEGF epitope was not found to be in the required α-helical conformation by circular dichroism and its overall in vitro bioactivity was not markedly different from an RGDS fibronectin epitope. This result suggests to us that perhaps the peptide is not acting in a truly VEGF-mimetic way when presented on these β-sheet ribbon assemblies, and could be instead acting as an extracellular matrix as opposed to a protein mimic. The studies we have described in this work, however, establish that the epitope is in its appropriate conformation when presented on our cylindrical nanofibers and also that this epitope specifically acts in a mimetic fashion by activating VEGF receptors. Presentation on highly hydrated cylindrical supramolecular assemblies could afford more dynamics for efficient and potent receptor-mediated signaling that may not be possible on flat ribbon-like assemblies. In addition to functional in vitro evaluations, we have gone well beyond this previous work in our use of two different in vivo models to establish angiogenic bioactivity and therapeutic efficacy.

There are several potential explanations underlying the enhanced epitope potency that we have demonstrated by our VEGF PA nanostructures compared to the soluble mimetic peptide control. As our CD melting curves established, the bioactive secondary structure of the epitope, an α-helix, is stabilized when incorporated within supramolecular aggregates of PA molecules. Stabilization of the bioactive conformation would likely translate into enhanced epitope bioactivity. The enhanced retention observed here could also explain in part the increased efficacy seen in vivo, though presumably retention would not be an issue for the short in vitro studies.

A feature of the PA that could enhance its bioactivity compared to the peptide control is the polyvalency of epitopes on the nanostructure surface. It is well established that polyvalency, the presentation of multiple bioactive binding sites, significantly enhances binding strength for biological interactions, a phenomenon known as avidity (38). This phenomenon has a natural basis, vital to the function of binding proteins such as IgM with 10 binding sites (39) or the biological adhesion of many viruses (40), and even the extracellular matrix is polyvalent (41). Polyvalency is used frequently in the design of synthetic bioactive molecules to enhance their binding strength and has been used in the creation of bioactive peptides, organic molecules, carbohydrates, nucleotides, antibiotics, and phage mimics, among others (42–46). Polyvalency has even been explored for biological signaling initiated by receptor dimerization, as is the case for VEGF receptor signaling. Examples include synthetic multivalent mimics of erythropoietin and thrombopoietin, both of which require receptor dimerization that is enhanced by multivalent signals (47, 48). Native VEGF, as a homodimeric cysteine knot protein, is multivalent (specifically divalent) with two bioactive domains that interact with receptor dimers (3), a feature that is not recreated in the soluble VEGF peptide mimic. The polyvalent and dynamic PA nanofiber could facilitate the necessary dimerization of receptors in a highly efficient manner. For the VEGF PA nanofibers investigated here, dynamic features of the nanostructures could help match the lengths necessary to promote receptor dimerization. PA nanostructures are highly hydrated, giving epitopes flexibility in both order and spacing within the assembled nanostructure. Given what is known about polyvalency in biological signaling, it is reasonable that avidity afforded by a dynamic PA assembly plays a role in the enhancement in bioactivity observed for the VEGF PA nanostructures relative to the soluble single peptide mimic. Regardless of the mechanistic details, because two bioactive signals must be present for VEGF receptor dimerization and activation, something which is the case for native VEGF protein with two cysteine-tethered bioactive domains, it is logical that PA molecules programmed for aggregation would be more apt to colocalize epitopes than would a soluble peptide, even if an enhanced avidity is not postulated.

As mentioned previously, some issues raised with the clinical application of VEGF or other recombinant proteins are specific target tissue retention, limited production resources, and cost. Bioactive PAs provide a potential means to overcome these obstacles, and we were especially encouraged that the VEGF PA compared favorably to a high dose of recombinant protein. Though PAs are biodegradable by design and thus will be eventually broken down into natural products, they have been shown here to remain in the ischemic tissue for over 2 wk after injection. This result is a substantial improvement when compared to the retention time reported for VEGF protein on the order of a few hours. Another possible consideration is cost, which has been speculated to be prohibitively expensive to the clinical implementation of efficacious protein-based therapies (4). The prolonged retention and bioavailability of the PA in the target tissue could address both of these issues, circumventing the need for serial protein deliveries and the additional pain and suffering, along with cost, entailed therein. In many ways, the therapeutic mechanism observed here for the PA could be similar to observations for biomaterials that facilitate the slow release of VEGF protein. Nanofiber geometry and dynamics make it unlikely that a high percentage of the total epitopes presented on the PA are signaling at any given time, which makes the exact bioactive dose of PA difficult to determine. However, increased retention and bioavailability allows for more continuous and lasting signaling of the epitopes presented on the PA and, as nanofibers break apart in vivo, smaller aggregates could diffuse and signal in the tissue surrounding the injection site. This effect is similar to a scaffold-based controlled release approach, except here the effect is achieved using a defined single component synthetic system that can be delivered by a minimally invasive injection, which is not the case for several of the polymeric growth factor delivery scaffolds reported to date. Overall, the results we have demonstrated for bioactivity and therapeutic efficacy of this proangiogenic PA designed to signal through VEGF receptors point to the translational potential of this strategy.

We have demonstrated that a polyvalent self-assembling nanofiber displaying a known VEGF mimicking sequence is efficacious in a hind-limb ischemia model of cardiovascular disease. The observed functional recovery is likely linked to

the proangiogenic, VEGF-mimetic behavior of the VEGF PA nanostructures established both in vitro and in vivo. Presentation of the mimetic epitope on the polyvalent nanofiber leads to more efficient and effective VEGF signaling compared to the bioactive peptide alone. Further, the PA compares favorably to a high-dose injection of recombinant protein. We conclude that these bioactive nanostructures are a promising synthetic therapeutic strategy to regenerate microcirculation and restore perfusion to ischemic tissue in cardiovascular diseases and could provide an alternative to VEGF protein-based strategies.

Materials and Methods

Detailed experimental methods can be found in the *SI Text*. Briefly, PAs and peptides for this study were synthesized by solid phase methods and purified by reversed phase HPLC. Nanofibers were imaged by cryogenic TEM, gels were imaged using SEM, and CD was preformed using standard methods. Primary HUVECs were purchased and used at passage 4. The receptor phosphorylation studies were performed using commercially available kits. Proliferation was assessed by a standard DNA-based assay, survival was assessed using flow cytometry, and migration was assessed by a scratch assay. The CAM assay was performed on fertilized chicken eggs, evaluating blood vessel density surrounding a coated coverslip in digital images captured through a microscope. The murine hind-limb ischemia model was performed in wild-type mice. The right femoral artery was ligated and excised, and the material was administered 3 d after induction of ischemia. Animals were scored on a semiquantitative scale for limb salvage (scale 1–6), motor function (scale 1–5), and were imaged by LDPI. Tissue perfusion is the ratio of ischemic to nonischemic limb perfusion from LDPI. Endurance testing was performed on a Rota Rod. At the end of the study, tissue was stained with antibodies to CD31 and smooth muscle actin and DAPI.

ACKNOWLEDGMENTS. The authors thank Dr. Yuri Velichko for assistance with molecular graphics. We gratefully acknowledge funding support from National Institutes of Health (NIH), specifically Award 1R01-EB003806-04 (to S.I.S.) and Awards HL-53354, HL-57516, HL-77428, HL-63414, HL-80137, and P01HL-66957 (to D.W.L.). This work was also supported by an Institute for Bionanotechnology in Medicine—Baxter Research Incubator Grant (J.T. and D.W.L.). Support for M.J.W. was provided by the Northwestern Regenerative Medicine Training Program NIH Award 5T90-DA022881 and support for J.T. by the German Heart Foundation, Solvay Pharmaceuticals, and the American Heart Association Midwest Affiliate. Peptide synthesis and purification was performed at the core facility of the Northwestern Institute for BioNanotechnology in Medicine. Instrumentation was used at the Northwestern Electron Probe Instrumentation Center (SEM), Biological Imaging Facility (TEM), and Keck Biophysics Facility (CD).

1. Lloyd-Jones D, et al. (2009) Heart disease and stroke statistics—2009 update: A report from the American Heart Association Statistics Committee and Stroke Statistics Subcommittee. *Circulation* 119:480–486.
2. Folkman J (2007) Angiogenesis: An organizing principle for drug discovery? *Nat Rev Drug Discov* 6:273–286.
3. Ferrara N, Gerber HP, LeCouter J (2003) The biology of VEGF and its receptors. *Nat Med* 9:669–676.
4. Gupta R, Tongers J, Losordo DW (2009) Human studies of angiogenic gene therapy. *Circ Res* 105:724–736.
5. Yla-Herttuala S, Rissanen TT, Vajanto I, Hartikainen J (2007) Vascular endothelial growth factors: Biology and current status of clinical applications in cardiovascular medicine. *J Am Coll Cardiol* 49:1015–1026.
6. Laham RJ, et al. (1999) Intracoronary and intravenous administration of basic fibroblast growth factor: Myocardial and tissue distribution. *Drug Metab Dispos* 27:821–826.
7. Lu E, et al. (2003) Targeted in vivo labeling of receptors for vascular endothelial growth factor: Approach to identification of ischemic tissue. *Circulation* 108:97–103.
8. Post MJ, Laham R, Sellke FW, Simons M (2001) Therapeutic angiogenesis in cardiology using protein formulations. *Cardiovasc Res* 49:522–531.
9. Hartgerink JD, Beniash E, Stupp SI (2001) Self-assembly and mineralization of peptide-amphiphile nanofibers. *Science* 294:1684–1688.
10. Hartgerink JD, Beniash E, Stupp SI (2002) Peptide-amphiphile nanofibers: A versatile scaffold for the preparation of self-assembling materials. *Proc Natl Acad Sci USA* 99:5133–5138.
11. Webber MJ, Kessler JA, Stupp SI (2010) Emerging peptide nanomedicine to regenerate tisues and organs. *J Intern Med* 267:71–88.
12. Cui H, Webber MJ, Stupp SI (2010) Self-assembly of peptide amphiphiles: From molecules to nanostructures to biomaterials. *Biopolymers* 94:1–18.
13. Webber MJ, et al. (2010) Development of bioactive peptide amphiphiles for therapeutic cell delivery. *Acta Biomater* 6:3–11.
14. Silva GA, et al. (2004) Selective differentiation of neural progenitor cells by high-epitope density nanofibers. *Science* 303:1352–1355.
15. Muraoka T, Koh CY, Cui H, Stupp SI (2009) Light-triggered bioactivity in three dimensions. *Angew Chem Int Ed Engl* 48:5946–5949.
16. Tovar JD, Claussen RC, Stupp SI (2005) Probing the interior of peptide amphiphile supramolecular aggregates. *J Am Chem Soc* 127:7337–7345.
17. Ghanaati S, et al. (2009) Dynamic in vivo biocompatibility of angiogenic peptide amphiphile nanofibers. *Biomaterials* 30:6202–6212.
18. Tysseling-Mattiace VM, et al. (2008) Self-assembling nanofibers inhibit glial scar formation and promote axon elongation after spinal cord injury. *J Neurosci* 28:3814–3823.
19. Webber MJ, et al. (2010) Capturing the stem cell paracrine effect using heparin-presenting nanofibres to treat cardiovascular diseases. *J Tissue Eng Regen Med* 4:600–610.
20. Chen RR, et al. (2007) Integrated approach to designing growth factor delivery systems. *FASEB J* 21:3896–3903.
21. Silva EA, Mooney DJ (2007) Spatiotemporal control of vascular endothelial growth factor delivery from injectable hydrogels enhances angiogenesis. *J Thromb Haemost* 5:590–598.
22. Silva EA, Mooney DJ (2010) Effects of VEGF temporal and spatial presentation on angiogenesis. *Biomaterials* 31:1235–1241.
23. Garbern JC, Hoffman AS, Stayton PS (2010) Injectable pH- and temperature-responsive poly(N-isopropylacrylamide-co-propylacrylic acid) copolymers for delivery of angiogenic growth factors. *Biomacromolecules* 11:1833–1839.
24. Tae G, Scatena M, Stayton PS, Hoffman AS (2006) PEG-cross-linked heparin is an affinity hydrogel for sustained release of vascular endothelial growth factor. *J Biomater Sci Polym Ed* 17:187–197.
25. Rajangam K, et al. (2006) Heparin binding nanostructures to promote growth of blood vessels. *Nano Lett* 6:2086–2090.
26. Zisch AH, et al. (2003) Cell-demanded release of VEGF from synthetic, biointeractive cell ingrowth matrices for vascularized tissue growth. *FASEB J* 17:2260–2262.
27. Zisch AH, Schenk U, Schense JC, Sakiyama-Elbert SE, Hubbell JA (2001) Covalently conjugated VEGF—fibrin matrices for endothelialization. *J Control Release* 72:101–113.
28. D'Andrea LD, Del Gatto A, Pedone C, Benedetti E (2006) Peptide-based molecules in angiogenesis. *Chem Biol Drug Des* 67:115–126.
29. Ferrara N, Kerbel RS (2005) Angiogenesis as a therapeutic target. *Nature* 438:967–974.
30. D'Andrea LD, et al. (2005) Targeting angiogenesis: Structural characterization and biological properties of a de novo engineered VEGF mimicking peptide. *Proc Natl Acad Sci USA* 102:14215–14220.
31. Diana D, et al. (2008) Structural determinants of the unusual helix stability of a de novo engineered vascular endothelial growth factor (VEGF) mimicking peptide. *Chemistry* 14:4164–4166.
32. Malkar NB, Lauer-Fields JL, Juska D, Fields GB (2003) Characterization of peptide-amphiphiles possessing cellular activation sequences. *Biomacromolecules* 4:518–528.
33. Matsumoto T, Claesson-Welsh L (2001) VEGF receptor signal transduction. *Sci STKE* 2001:re21.
34. Duval M, Bedard-Goulet S, Delisle C, Gratton JP (2003) Vascular endothelial growth factor-dependent down-regulation of Flk-1/KDR involves Cbl-mediated ubiquitination. Consequences on nitric oxide production from endothelial cells. *J Biol Chem* 278:20091–20097.
35. Yancopoulos GD, et al. (2000) Vascular-specific growth factors and blood vessel formation. *Nature* 407:242–248.
36. Kofidis T, et al. (2002) Restoration of blood flow and evaluation of corresponding angiogenic events by scanning electron microscopy after a single dose of VEGF in a model of peripheral vascular disease. *Angiogenesis* 5:87–92.
37. Wang X, Horii A, Zhang S (2008) Designer functionalized self-assembling peptide nanofiber scaffolds for growth, migration, and tubulogenesis of human umbilical vein endothelial cells. *Soft Matter* 4:2388–2395.
38. Vance D, Martin J, Patke S, Kane RS (2009) The design of polyvalent scaffolds for targeted delivery. *Adv Drug Deliv Rev* 61:931–939.
39. Czajkowsky DM, Shao Z (2009) The human IgM pentamer is a mushroom-shaped molecule with a flexural bias. *Proc Natl Acad Sci USA* 106:14960–14965.
40. Douglas T, Young M (2006) Viruses: Making friends with old foes. *Science* 312:873–875.
41. Hynes RO (2009) The extracellular matrix: Not just pretty fibrils. *Science* 326:1216–1219.
42. Galeazzi S, et al. (2009) Multivalent supramolecular dendrimer-based drugs. *Biomacromolecules* 11:182–186.
43. Mammen M, Choi SK, Whitesides GM (1998) Polyvalent interactions in biological systems: Implications for design and use of multivalent ligands and inhibitors. *Angew Chem Int Ed Engl* 37:2755–2794.
44. Rao J, Lahiri J, Isaacs L, Weis RM, Whitesides GM (1998) A trivalent system from vancomycin. D-ala-D-Ala with higher affinity than avidin.biotin. *Science* 280:708–711.
45. Helms BA, et al. (2009) High-affinity peptide-based collagen targeting using synthetic phage mimics: From phage display to dendrimer display. *J Am Chem Soc* 131:11683–11685.
46. Vance D, Shah M, Joshi A, Kane RS (2008) Polyvalency: A promising strategy for drug design. *Biotechnol Bioeng* 101:429–434.
47. Cwirla SE, et al. (1997) Peptide agonist of the thrombopoietin receptor as potent as the natural cytokine. *Science* 276:1696–1699.
48. Johnson DL, et al. (1997) Amino-terminal dimerization of an erythropoietin mimetic peptide results in increased erythropoietic activity. *Chem Biol* 4:939–950.